

**$^{100}\text{Sn}$  core excitations in  $^{97}\text{Ag}$** M. Lipoglavšek,<sup>1,\*</sup> M. Vencelj,<sup>1</sup> C. Baktash,<sup>2</sup> P. Fallon,<sup>3</sup> P. A. Hausladen,<sup>2</sup> A. Likar,<sup>1,4</sup> and C.-H. Yu<sup>2</sup><sup>1</sup>*Jozef Stefan Institute, 1000 Ljubljana, Slovenia*<sup>2</sup>*Physics Division, Oak Ridge National Laboratory, Oak Ridge, Tennessee, USA*<sup>3</sup>*Lawrence Berkeley National Laboratory, Berkeley, California, USA*<sup>4</sup>*Faculty of Mathematics, Physics, University of Ljubljana, Slovenia*

(Received 28 September 2005; published 29 December 2005)

Excited states of  $^{97}\text{Ag}$ , which has three protons less than doubly magic  $^{100}\text{Sn}$ , were identified up to 7 MeV excitation energy and  $J = (33/2)$ . The reaction  $^{46}\text{Ti} + ^{58}\text{Ni}$  was employed together with the Gammasphere Ge detector array coupled with Microball and Neutron Shell auxiliary detectors. The measured states are compared with a large-scale shell-model calculation.

DOI: [10.1103/PhysRevC.72.061304](https://doi.org/10.1103/PhysRevC.72.061304)

PACS number(s): 21.10.-k, 21.60.Cs, 23.20.Lv, 27.60.+j

The self-conjugate doubly magic nucleus  $^{100}\text{Sn}$  has lately drawn much attention from nuclear physicists. However, it remains elusive, and we have to infer its structure by studying excited states of neighboring nuclei. Nuclei closest to  $^{100}\text{Sn}$  with experimentally determined excited states are currently the  $T_z = 1$  nuclei  $^{102}\text{Sn}$  [1] and  $^{98}\text{Cd}$  [2] and the  $T_z = 3/2$  nuclei  $^{103}\text{Sn}$  [3],  $^{101}\text{In}$ ,  $^{99}\text{Cd}$  [4], and  $^{97}\text{Ag}$  [5]. We report here the first spectroscopic information on  $^{100}\text{Sn}$  core excited states in  $^{97}\text{Ag}$  including a core excited isomeric level. Data are compared with large-scale shell-model calculations using an effective interaction derived from the nucleon-nucleon interaction.

The experiment was performed at the 88" cyclotron at Lawrence Berkeley National Laboratory by using the Gammasphere Ge detector array [6] together with the Microball light charged particle [7] and the Neutron Shell neutron detector arrays [8]. The cyclotron delivered a 175 MeV  $^{46}\text{Ti}$  beam that impinged on a 2 mg/cm<sup>2</sup> thick  $^{58}\text{Ni}$  target backed with 10 mg/cm<sup>2</sup> gold. Gammasphere comprised 78 BGO-shielded Ge detectors, since the forward  $1\pi$  detector solid angle was filled with 30 liquid scintillator neutron detectors. Microball, placed inside the Gammasphere scattering chamber, consisted of 95 CsI(Tl) scintillators for the detection of evaporated protons and  $\alpha$  particles. The trigger system required two BGO-unsuppressed Ge signals within 800 ns after the time of reaction, which was determined by an overlap of Ge and cyclotron radiofrequency signals. In addition, the trigger system required the detection of at least one neutron, which was discriminated on line from  $\gamma$  rays also detected in neutron detectors. On-line neutron- $\gamma$  discrimination was done with the time-of-flight method.

Off-line neutron- $\gamma$  discrimination was done with a combination of pulse height, time-of-flight, and slow scintillation light component signals. In this way a relatively high neutron detection efficiency of 21% was preserved, and at the same time very few, less than 1%, of events not connected with neutron emission ended up in neutron gated spectra. Protons and  $\alpha$  particles detected in Microball were off-line distinguished from each other according to a combination of

detector pulse height, time, and shape. This yielded proton and  $\alpha$ -particle detection efficiencies of 80% and 46%, respectively. Because of the overlap of protons and  $\alpha$  particles in detectors at backward angles, 18% of  $\alpha$  particles were misinterpreted as protons. On the other hand, only 0.2% of protons were misinterpreted as  $\alpha$  particles. This is important, since weakly populated reaction channels including  $\alpha$ -particle emission lead to more neutron-deficient nuclei. In this way,  $\alpha$ -particle gated  $\gamma$ -ray spectra remain clean.

The nucleus described in this paper,  $^{97}\text{Ag}$ , was produced by evaporation of a proton, an  $\alpha$  particle, and two neutrons from the compound nucleus  $^{104}\text{Sn}$  with a cross section of about 0.5 mb [9]. Gamma rays belonging to  $^{97}\text{Ag}$  are shown in Fig. 1 and listed in Table I. The spectrum in Fig. 1 was constructed by requiring  $\gamma$  rays to be detected simultaneously with previously known 763 or 1290 keV  $\gamma$  rays and with one  $\alpha$  particle, one proton, and at least one neutron. An additional requirement was that all  $\gamma$  rays, including those used for gating, were detected between 9 and 38 ns after the time of reaction, which was determined by the cyclotron radio-frequency signal. This latter requirement eliminated the relatively strong 467 keV  $\gamma$  ray from the spectrum. Gamma-ray energies, intensities, angular distribution coefficients  $A_2$ , and transition initial and final states are listed in Table I for all transitions identified in  $^{97}\text{Ag}$  by  $\gamma$ - $\gamma$  coincidence relations. Angular distributions were fitted to  $\gamma$ -ray intensities detected in detectors placed at 9 different polar angles. Because of limited statistics only the  $A_2$  angular distribution coefficient was fitted. The level scheme shown in Fig. 2 was constructed on the basis of the following arguments. The 467 keV  $\gamma$  ray is the only one without a delayed component. This undoubtedly places it above both isomeric states. The ordering of  $\gamma$  rays between both isomeric states is well established owing to the cross-over transitions, except for the 2909 and 980 keV  $\gamma$  rays, which have identical intensities. They both show a delayed component, and the coincidence relationships place them in a cascade above the 2343 keV state. The 980 keV transition was placed above the 2909 keV one, because it would be difficult to explain weak population of a low-lying  $23/2^+$  state. Owing to the spin gap of  $3\hbar$ , the 6232 keV level cannot be fed directly from the second observed isomeric state, but only through unobserved levels lying between them. This implies that at

\*Electronic address: [matej.lipoglavsek@ijs.si](mailto:matej.lipoglavsek@ijs.si)

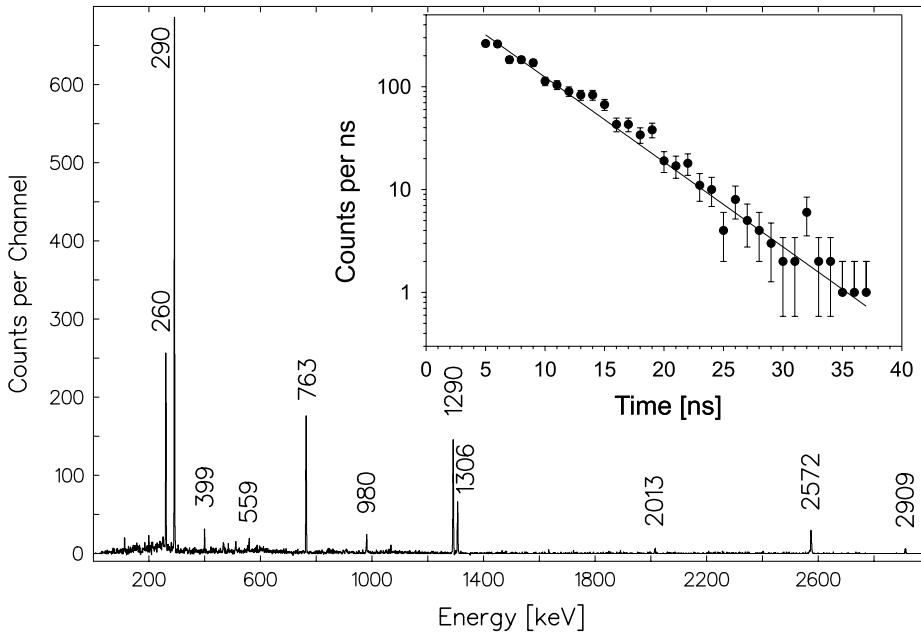


FIG. 1. A  $\gamma$ -ray spectrum, showing  $\gamma$  rays coincident with the 1290 or 763 keV transitions. Additional constraints are simultaneous detection of one  $\alpha$  particle, one proton, and at least one neutron and the detection of all  $\gamma$  rays within a time window between 9 and 38 ns after the reaction. The inset shows a time spectrum of the 2572 keV  $\gamma$  ray.

least two transitions with a summed energy of 249 keV were unobserved. A candidate for one of them is a transition at 112 keV, also visible in Fig. 1. This nonobservation is possible, because of the low detection efficiency at low  $\gamma$ -ray energy, since the relatively thick Microball detectors are placed in the  $\gamma$ -ray path.

The ordering of the lowest three transitions was preserved from Ref. [5]. Since the ground state spin and parity have not been measured, all spin-parity assignments in the level scheme are tentative. The ground state spin and parity were assumed to be  $(9/2^+)$ , in agreement with the previous proposal [5] and the  $\beta$ -decay results [10]. Positive parity was assumed for all states. No high-spin negative parity states are expected to lie near the yrast line. The negative parity  $h_{11/2}$  orbit is more than 2 MeV above the  $d_{5/2}$  and  $g_{7/2}$  orbits just across the shell

TABLE I. Energies, relative intensities and angular distribution coefficients  $A_2$  for transitions belonging to  $^{97}\text{Ag}$ . Transition initial and final state assignments are also shown.

Energy [keV]	Intensity	$A_2$	$J^\pi$ Initial	$J^\pi$ Final
260.2(3)	48(7)	0.61(16)	$(31/2^+)$	$(27/2^+)$
290.4(3)	93(13)	0.50(13)	$(21/2^+)$	$(17/2^+)$
399(1)	6(1)		$(27/2^+)$	$(25/2^+)$
467.1(3)	35(5)	-0.1(3)	$(33/2^+)$	$(31/2^+)$
559(1)	3(1)		$(23/2^+)$	$(21/2^+)$
763.0(2)	92(13)	0.24(6)	$(17/2^+)$	$(13/2^+)$
906.6(8)	5(2)		$(25/2^+)$	$(23/2^+)$
980.0(5)	17(3)	-0.9(4)	$(25/2^+)$	$(23/2^+)$
1289.9(2)	100(15)	0.35(2)	$(13/2^+)$	$(9/2^+)$
1306.0(3)	51(7)	0.57(12)	$(27/2^+)$	$(23/2^+)$
1466(1)	2(1)		$(25/2^+)$	$(21/2^+)$
2012.6(8)	9(2)	0.3(3)	$(21/2^+)$	$(21/2^+)$
2571.9(5)	55(9)	-0.81(9)	$(23/2^+)$	$(21/2^+)$
2909(1)	15(3)	-0.6(3)	$(23/2^+)$	$(21/2^+)$

gap. Negative parity states based on the  $p_{1/2}$  proton orbit are nonyrast, as well, with the  $17/2^-$  state calculated, as described below, at 2829 keV and the  $29/2^-$  state at 6937 keV coming closest to the yrast line. Moreover, no yrast negative parity high-spin states are known in neighboring  $^{98}\text{Cd}$  [2],  $^{99}\text{Cd}$  [4],  $^{98}\text{Ag}$  [11] and  $^{96}\text{Pd}$  [12] nuclei. The level spin assignments were determined according to angular distribution coefficients  $A_2$  (see Table I), assuming that transitions with positive  $A_2$  are quadrupole and those with negative  $A_2$  have a dipole character. It was also assumed that all transitions change level spins by the maximally allowed value. The large error bar for the  $A_2$  coefficient of the 467 keV transition allows for both dipole and quadrupole characters. The angular distribution for this  $\gamma$  ray requires a fit of the  $A_4$  coefficient, as well, suggesting a mixed  $M1/E2$  character, and hence a  $J^\pi = (33/2^+)$  assignment for the highest observed level. The angular distribution of the 2013 keV  $\gamma$  ray is consistent with a  $\Delta J = 0$  dipole transition. In contrast to the three lowest lying transitions, which are consistent with the level scheme of Ref. [5], the 260 keV transition was placed much higher in the level scheme, since many new transitions were found and were placed between the two identified isomeric states. Inspection of the spectra of Ref. [5] also shows the 1306 keV line, which remained unassigned at that time. The  $(21/2^+)$  level at 2343 keV was previously known to be isomeric, but its half-life could not be properly measured owing to the existence of a second isomeric state. We have identified this state and placed it at 6481 keV excitation energy. Its half-life was determined to be 3.7(1) ns from the fit of the time distributions of the 2572 and 1306 keV transitions. The former is shown as an inset in Fig. 1. The half-life of the 2343 keV level was determined to be 1.8(5) ns with a centroid shift method from the time differences of any combination of 1290 and 763 keV  $\gamma$  rays with 2572 and 1306 keV  $\gamma$  rays (Fig. 3).

To help interpret the measured level parameters, a large-scale shell-model calculation was performed. The calculation used  $^{78}\text{Sr}$  as a core and an effective interaction based on the



promoted from the  $g_{9/2}$  to the  $d_{5/2}$  orbit. The same happens in the second  $23/2^+$  and in the lowest lying  $25/2^+$  level, while in the lowest lying  $23/2^+$  and  $27/2^+$  and in the second  $25/2^+$  state the neutron is predominantly in the  $g_{7/2}$  orbit. The wave function of the isomeric  $31/2^+$  level has a similar neutron  $d_{5/2}$  and  $g_{7/2}$  occupation probability, and in the  $33/2^+$  state the neutron is again predominantly in the  $d_{5/2}$  orbit. All other occupation numbers remain almost the same for all core excited states. The structure of the  $23/2^+$  state, through which the main core deexcitation proceeds, can be qualitatively understood due to the strong attraction of the aligned proton and neutron holes. The  $g_{7/2}$  neutron anti aligns to the aligned  $(\pi g_{9/2}^{-3} \nu g_{9/2}^{-1})_{15^+}$  configuration, resulting in  $J^\pi = 23/2^+$ . A similar configuration involving a  $d_{5/2}$  neutron gives  $J^\pi = 25/2^+$ , explaining the alternating occupation numbers of the core excited states.

The calculation correctly predicts the existence of both observed isomeric states by placing the lowest  $19/2^+$  level above the  $21/2^+$  one and the  $29/2^+$  above the isomeric  $31/2^+$  level. The  $21/2^+$  level is a seniority isomer, while the  $31/2^+$  level is a spin gap isomer due to the strong  $g_{9/2}$  proton-neutron hole-hole interaction, similar to the  $15^+$  isomer in  $^{96}\text{Pd}$  [12].

The experimental reduced transition probability for the  $21/2^+ \rightarrow 17/2^+$  transition is 5.6 W.u.(Weisskopf units). This value is more than a factor of 2 higher than the one calculated in Ref. [15], where the effective interaction was derived in a similar way to our calculation. However, Coraggio *et al.* [15] used an effective proton charge of  $1.35e$  and limited the valence nucleons to protons only. It is known that the effective operator used in Ref. [15] gives rather low  $B(E2)$  values. An  $e_{\text{eff}}(\pi) = 2.0e$  was, therefore, used in a similar but more recent calculation for the even- $A$ ,  $N = 50$  isotones in Ref. [16]. The 4.6 W.u. reduced transition probability for the  $31/2^+ \rightarrow 27/2^+$  transition may be, at first glance surprisingly lower than the one for the  $21/2^+ \rightarrow 17/2^+$  transition. On the other hand, this may also show that even at 6.5 MeV excitation energy,  $^{97}\text{Ag}$  is still a good shell-model nucleus without much collective

motion. The situation is similar in the neighboring  $N = 50$  isotone  $^{96}\text{Pd}$ , where the  $15^+ \rightarrow 13^+$  transition is relatively slower than the  $8^+ \rightarrow 6^+$  one. Since there are two isomeric states in  $^{97}\text{Ag}$ , we were able to deduce both proton and neutron effective charges. Both measured reduced transition probabilities are simultaneously explained by using  $e_{\text{eff}}(\pi) = 1.9(5)e$  and  $e_{\text{eff}}(\nu) = 1.1(8)e$  in our shell-model calculation. These values are reasonable but relatively large for a nucleus that close to a double shell closure. This may show that the  $^{100}\text{Sn}$  core, like  $^{56}\text{Ni}$ , is not very rigid, or it may be the first indication that the model space used in the calculation is too small. Despite taking into account neutron excitations across the  $N = 50$  shell gap, our shell-model calculation remains highly truncated, and it is known that such calculations give effective charges that are too large. There are indications of a large  $e_{\text{eff}}(\nu) > \approx 2e$  already from the measured half-life of the  $6^+$  state in  $^{102}\text{Sn}$  [1] calculated with a truncated model space. It has been shown [17] that more reasonable polarization charges of about  $0.5e$  can explain the measured  $B(E2)$  value in  $^{102}\text{Sn}$  when core excitations are explicitly included in the model space. Note that, because of the large uncertainty of the measured half-life of the  $21/2^+$  state, the effective charges are not well determined. This is especially true for the neutron effective charge.

It should be pointed out that, in contrast to  $^{99}\text{Cd}$ ,  $^{101}\text{In}$ , and  $^{98}\text{Ag}$ , where lowest core excited states decay by strong  $E2$  transitions, the main core deexcitation proceeds with a high energy dipole transition, similar to the situation in neighboring  $^{96}\text{Pd}$  and in  $^{53}\text{Mn}$  [18], the three proton hole nucleus in the  $^{56}\text{Ni}$  region. This is another similarity between the two self-conjugated doubly magic nuclei  $^{100}\text{Sn}$  and  $^{56}\text{Ni}$ , corroborating the prediction of a low-lying  $2^+$  state in  $^{100}\text{Sn}$ .

Oak Ridge National Laboratory is operated by UT-Battelle, LLC for the U.S. Department of Energy(DOE) under contract No. DE-AC05-00OR22725. Work at Lawrence Berkley National Laboratory is supported in part by the U.S. DOE under contract DE-AC03-76SF00098.

- 
- [1] M. Lipoglavšek *et al.*, Phys. Lett. **B440**, 246 (1998).  
 [2] A. Blazhev *et al.*, Phys. Rev. C **69**, 064304 (2004).  
 [3] C. Fahlander *et al.*, Phys. Rev. C **63**, 021307(R) (2001).  
 [4] M. Lipoglavšek *et al.*, Phys. Rev. C **66**, 011302(R) (2002).  
 [5] D. Alber *et al.*, Z. Phys. A **335**, 265 (1990).  
 [6] I. Y. Lee, Nucl. Phys. A **520**, 641c (1990).  
 [7] D. G. Sarantites *et al.*, Nucl. Instrum. Methods Phys. Res. A **381**, 418 (1996).  
 [8] D. G. Sarantites *et al.*, Nucl. Instrum. Methods Phys. Res. A **530**, 473 (2004).  
 [9] M. Vencelj *et al.*, Phys. Scr. (in press).  
 [10] Z. Hu *et al.*, Phys. Rev. C **60**, 024315 (1999).  
 [11] M. Vencelj *et al.* (in preparation); M. Vencelj, M.S. Thesis, University of Ljubljana.  
 [12] D. Alber *et al.*, Z. Phys. A **332**, 129 (1989).  
 [13] R. Machleidt, F. Sammarruca, and Y. Song, Phys. Rev. C **53**, R1483 (1996).  
 [14] T. Engeland, M. Hjorth-Jensen, and E. Osnes, Phys. Rev. C **61**, 021302(R) (2000).  
 [15] L. Coraggio *et al.*, J. Phys. G **26**, 1697 (2000).  
 [16] A. F. Lisetskiy, B. A. Brown, M. Horoi, and H. Grawe, Phys. Rev. C **70**, 044314 (2004).  
 [17] F. Nowacki, Nucl. Phys. A **704**, 223c (2002).  
 [18] P. Banerjee, B. Sethi, M. B. Chatterjee, and R. Goswami, Phys. Rev. C **44**, 1128 (1991).